

Research article

Wenhui Wang, Ruxia Du, Litao Sun, Wei Chen, Junpeng Lu and Zhenhua Ni*

Ultrasensitive graphene position-sensitive detector induced by synergistic effects of charge injection and interfacial gating

<https://doi.org/10.1515/nanoph-2020-0053>

Received January 24, 2020; revised February 24, 2020; accepted February 25, 2020

Abstract: Position-sensitive detectors (PSDs) are essential components to the realization of displacement and vibration detection, optical remote control, robot vision, etc. The light sensitivity of PSDs is a crucial parameter, which determines the operating range or detection accuracy of the measurement systems. Here, we devise an ultrasensitive PSD based on graphene/Si hybrid structure by using the synergistic effect of charge injection and interfacial gating. Photogenerated carriers in Si are separated by the built-in electric field at the surface. Holes diffuse laterally in inversion layer and then inject into graphene to form photoresponse. Meanwhile, the electrons in bulk Si that move to the area under graphene cause a gating effect, thus introducing a high gain. With the benefit of synergistic effect, the detection limit power of our device can be pushed to pW level, which is reduced by two orders of magnitude compared to previously reported graphene based PSD. Furthermore, even for infrared light of 1064 nm, the

PSD still retains position sensitivity to 1 nW weak light, as well as fast response speed at the μs level. This work provides the potential of graphene as a promising material for ultraweak light position sensitive detection.

Keywords: graphene; charge injection; interfacial gating; position-sensitive detector.

1 Introduction

Position-sensitive detector (PSD), a kind of optical inspection systems for the precise measurement of position, distance, displacement, angle, and other relevant physical variables, is a crucial component for diverse applications, including optical engineering, aerospace, real-time tracking and nanorobotics [1–4]. In tracking or remote measurement systems, high sensitivity and ultra-weak light detection capability are crucial, which determine the accuracy and operating distance of the systems. Heterojunction structures, including silicon (Si) P-N or P-I-N junctions [5, 6], and metal-Si Schottky junctions [7–10], are the most common structures for current PSD. The sensitivity of these devices is still not satisfactory and they normally operate under μW or mW incident light. In addition, for the purposes of eye safety and concealment, the infrared light is the routine operating wavelength for sensing systems, which is also a bottleneck for PSD based on these structures due to the weak light absorption and lack of gain. Recently, by virtue of the excellent properties, various two-dimensional materials have been employed to fabricate PSDs and some new structures were proposed [11–16]. In our previous studies, we designed a graphene-based PSD using interfacial amplification [15], and its detection limit power can be reduced to nW level by introducing gain. However, detection of weaker light (pW level ultraweak light) is still desirable, because it implies greater accuracy and precision. Moreover, the infrared detection capability of PSDs also needs to be further improved. Therefore, it is significant to continue to low

*Corresponding author: **Zhenhua Ni**, School of Physics and Key Laboratory of MEMS of the Ministry of Education, Southeast University, Nanjing 211189, China, e-mail: zhni@seu.edu.cn. <https://orcid.org/0000-0002-6316-2256>

Wenhui Wang: School of Physics and Key Laboratory of MEMS of the Ministry of Education, Southeast University, Nanjing 211189, China; and Centre for Functional Materials, National University of Singapore (Suzhou) Research Institute, Suzhou 215123, China

Ruxia Du: Department of Basic Teaching, Nanjing Tech University Pujian Institute, Nanjing 211134, China

Litao Sun: SEU-FEI Nano-Pico Center, Key Laboratory of MEMS of Ministry of Education, Collaborative Innovation Center for Micro/Nano Fabrication, Device and System, Southeast University, Nanjing 210096, China

Wei Chen: Centre for Functional Materials, National University of Singapore (Suzhou) Research Institute, Suzhou 215123, China; and Department of Chemistry, National University of Singapore, 3 Science Drive 3, Singapore 117543, Singapore

Junpeng Lu: School of Physics and Key Laboratory of MEMS of the Ministry of Education, Southeast University, Nanjing 211189, China

down the detection limit power and realize the ultraweak light position detection.

In conventional heterojunction based PSDs, separated photogenerated holes (electrons) diffuse laterally in the surface layer to form photoresponse. While in our previously reported PSD based on interfacial amplification effect, photogenerated electrons at the interface of SiO_2/Si cause a gating effect and a high photoresponse. For both of them, only one type of carrier (electron or hole) contributes to photoresponse and position sensitivity [12–17]. Here, we present an ultrasensitive graphene based PSD on lightly n-doped Si substrate by using synergistic effect of charge injection and interfacial gating. Both photo-induced holes and electrons are involved and contribute to the PSD performance. Due to the synergistic effect, the detection limit power of the PSD has been pushed to ~ 10 pW, which is two orders of magnitude lower than that of previous PSD. In addition, it is worth noting that, even for infrared light of 1064 nm, the PSD still retains position sensitivity to 1 nW weak light. Meanwhile, the PSD possesses fast response speed at the μs level. The outstanding performance combined with simple fabrication and compatibility with silicon technology let this device has an important development potential.

2 Materials and methods

The Si employed in the experiment was lightly n-doped with resistivity of 1–10 Ω cm. The surface impurities and oxide layers of the Si were first removed by hydrofluoric acid, followed by cleaning the Si with acetone, ethanol, and deionized water in order. Then, the Si was placed in a drying oven at room temperature for 2 h to form a uniform native oxide layer on the surface. The mechanically exfoliated graphene was deposited on the Si substrate, and then the source and drain electrodes (Ni (5 nm)/

Au (50 nm)) were patterned by electron-beam lithography (FEI, FP2031/12 INSPECT F50), thermal evaporation (TPRE-Z20-IV), and lift-off processes. Electrical, photoelectric data and position sensitive characteristics of the PSD were measured using a Keithley 2612 analyzer. The light source was a femtosecond laser (Chameleon Ultra II), which can obtain different wavelength lasers by modulating the optical parametric oscillators. In the response speed measurement, light was modulated by an acoustic optical modulator (R21080-1DS) with frequency of 1 kHz. A digital storage oscilloscope (Tektronix TDS 1012) was used to measure the transient response. All the measurements were performed in air at room temperature.

3 Results and discussion

3.1 High photoresponse of graphene device

The representative schematic of our device was shown in Figure 1A, which is a two-terminal graphene device (the channel is 15 μm in length, 8 μm in width) deposited on the lightly n-doped Si substrate. The Raman spectrum shows that it is a few-layer graphene flake (See Supplementary Material Figure S1). The I–V curve of this device demonstrates the higher conductivity of graphene as compared to the Si substrate, indicating that the current is mainly transported in graphene channel (Figure S2). The photoresponse characteristics of the device were recorded with laser focused on the edge of graphene channel ($X=0$ μm), where the laser wavelength was 532 nm and the spot size was ~ 1.5 μm . As shown in Figure 1B, the device exhibits fast and high photoresponse capability, which could respond to weak light as low as 0.4 pW. The obtained photoresponsivity has reached nearly $\sim 10^6$ A/W

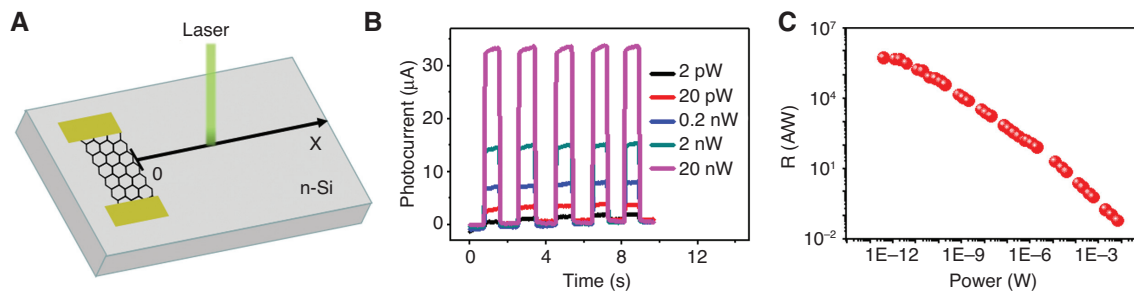


Figure 1: Photoresponse of the graphene device.

(A) Schematic view of the graphene devices on lightly n-doped Si. X represents the distance of the laser illumination position from the graphene channel. (B) Photo-switching characteristics and (C) photoresponsivity of the device act as a photodetector at different power ($X=0$ μm , $V_{\text{ds}}=1$ V).

(Figure 1C), which is comparable to that of graphene-Si heterojunction photodetectors reported previously. This high photoresponsivity is ascribed to the high mobility of graphene and absorption of Si, as well as the presence of a high gain of more than 10^4 in graphene-Si hybrid structure devices [15, 18, 19]. Recently, the graphene-Si hybrid structure has attracted great attention in practical applications, including solar cell [20–22], array imaging [23], etc. Here we mainly focus on the photoresponse outside the graphene channel, that is, the position-sensitive photoresponse characteristic. The high photoresponse performance suggests promising potential of our graphene device for ultrasensitive position detection.

3.2 Position-sensitive characteristics of the device

The photoresponse was collected at different distances (different X labeled in Figure 1A) from the graphene channel. Figure 2A shows typical photo-switching characteristics of the device under different position. It can be seen that a considerable photocurrent generates and its magnitude declines significantly with increasing the distance, implying excellent position sensitivity of the device. This also implies that our device can be acted as a PSD capable of detecting the position of ultraweak light

(pW level). The observed lateral photoeffect can be attributed to the presence of a built-in electric field at the surface of Si substrate, which will be discussed in detail later. To investigate the position sensitive characteristics, the photocurrent as a function of position at different power was displayed in Figure 2B. We note that, even at ultraweak incident power of 10 pW, the device still displays excellent position sensitive response, suggesting ultrasensitive property of our device to weak light signal. In addition, the power response range of the device cover from pW to mW, and the detection distance can reach mm level for uW and mW light, enhancing potential of our device for promising application. To prove the role of graphene in the device, control experiments were carried out. A pure Si device with the same channel length was fabricated, and the position sensitive characteristic was conducted. Although pure Si devices also have photoresponse capability and position sensitive characteristics, they require strong incident power above μW level. The photocurrent of pure Si device drops rapidly from 32 nA to zero at $\sim 30 \mu\text{m}$ under incident light of $10 \mu\text{W}$ which is negligible compared to the photoresponse of graphene device on Si (Figure 2C). It is high mobility of graphene and structure design that makes our device as a promising ultrasensitive PSD. Furthermore, the detection capability of the device can be modulated by bias to further improve (Figure S3). Spatial position resolution was also calculated by considering the

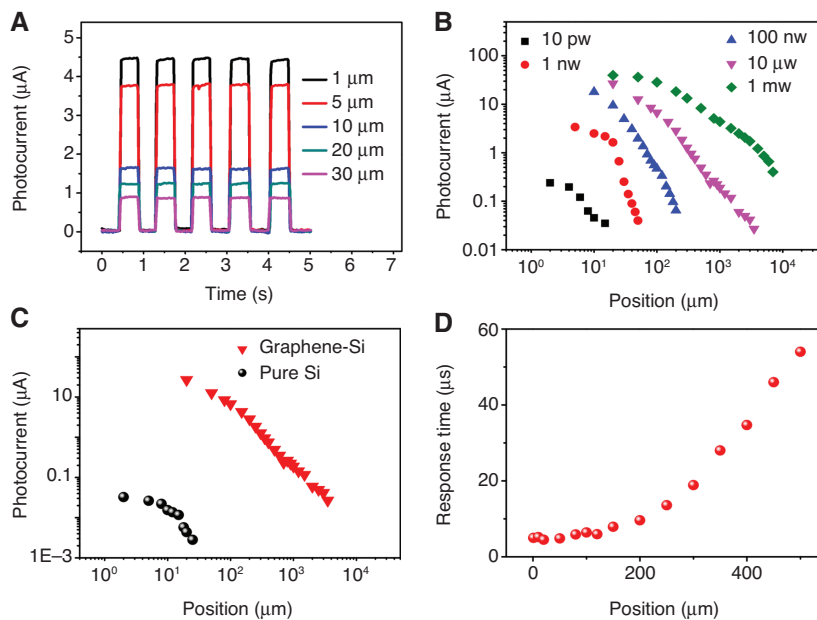


Figure 2: Position-sensitive characteristics of the device.

(A) Photo-switching characteristics of the device at different position (532 nm laser, $V_{ds} = 0.1 \text{ V}$) (B) Photocurrent as a function of position under different incident light powers. (C) The comparison of the position sensitive characteristics of the graphene-Si and pure Si devices under $10 \mu\text{W}$. (D) The position dependence of response time of the device.

detection limit of photocurrent, which was less than $1\ \mu\text{m}$ (Figure S4).

Next, the response speed of the device was studied and response time was obtained by fitting the transient response using a single exponential function (Figure S5). The position dependence of response time was shown in Figure 2D. The increase of response time with distance could be understood as the increase of transit time of the carriers from light spot to the graphene channel. Despite the increase, the response time is in the tens of microseconds, which enables the PSD to achieve high frequency (up to $\sim 10\ \text{kHz}$) detecting.

3.3 High performance of the PSD in near-infrared range

Infrared sensitivity is an important property of PSD for the eye safety and concealment. To prove the capability of our PSD, the position sensitive characteristics under $800\ \text{nm}$, $950\ \text{nm}$, $1064\ \text{nm}$ were recorded, as shown in Figure 3A. It can be seen that the photoresponse changes significantly with position, indicating excellent position sensitivity under infrared light. Figure 3B shows the spatial position resolution of the PSD as a function of power. The resolution gradually improves as the power increases, and reaches to tens of nanometers. More important, even for the infrared light of $1064\ \text{nm}$, the detection limit power of our PSD can still be $\sim 1\ \text{nW}$. The ultrasensitive performance of the PSD for visible-near infrared will enable the PSD to work under complex environment.

3.4 Mechanism for ultrasensitive graphene PSD

In order to better understand the ultrasensitive PSD, we proposed a synergistic effect mechanism model. Many

studies have confirmed the presence of charged surface states in lightly doped semiconductors, which is due to the dangling bonds, surface reconstruction, adsorbed ions, etc [24–26]. The surface states with donor or acceptor levels in the band gap will be emptied and filled through carrier dynamic process. Consequently, surface bands bending and a built-in electric field forms, generating depletion layer as well as an inversion layer. The inversion layer can provide a high speed path for carrier transport, which has been confirmed by previous studies [13, 14, 27–29]. For lightly n-doped Si, the surface bands bend upwards, leading to the electric field directing from bulk Si to the surface (Figure 4). Under illumination, the generated electron-hole pairs are separated by the built-in electric field. Holes will drift to the surface, while electrons will move into bulk Si. The holes then diffuse laterally in the inversion layer until they are recombined or transfer to graphene channel to form photocurrent. It is worth noting that the native oxide layer (between the inversion layer and graphene channel), which is generally $1\text{--}2\ \text{nm}$ thick, allows holes to tunnel through it quite freely [30] and therefore does not affect injection. However, the collection of holes is not sufficient to produce such a high photoresponse in our device. As can be seen from the comparison results in Figure 2C, the number of holes diffused into the channel should be the same under the same operating conditions, but the photoresponse of pure Si devices is much lower than that of graphene-Si structures. It is suggested that another photoresponse mechanism should exist.

Another potential contributor to the photoresponse is the electrons in bulk Si. The electrons can also diffuse laterally inside the Si [25], and the existence of the built-in electric field can effectively suppress the recombination of electrons in the bulk Si and holes in the inversion layer during diffusion. When the distribution of carrier

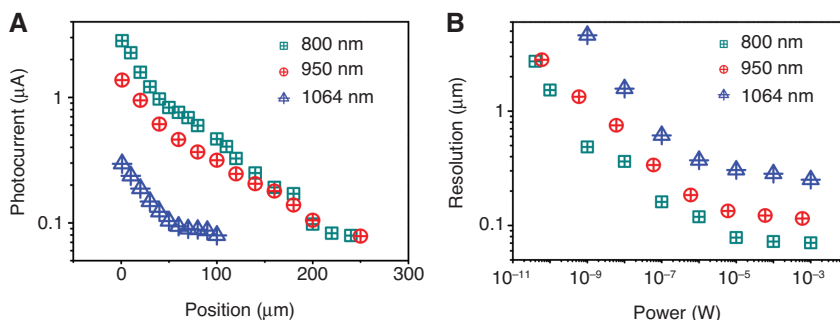


Figure 3: Infrared performance of the PSD.

(A) Position dependence of photocurrent of the PSD at infrared light of $800\ \text{nm}$, $950\ \text{nm}$, $1064\ \text{nm}$. (B) The spatial position resolution of the PSD as a function of power.

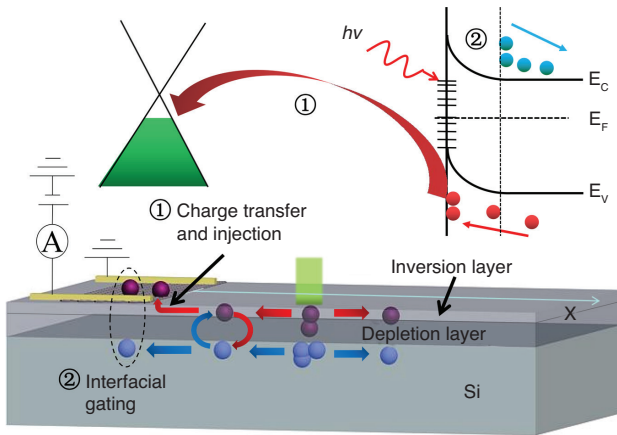


Figure 4: Energy band and carrier dynamics of the PSD.

The photo-induced holes drift to the surface of Si under the built-in electric field, which is followed by diffusion laterally in the inversion layer and injection into the graphene. While the electrons in bulk Si move to the region under graphene, which will cause interfacial gating effect.

reaches a dynamic equilibrium, the electrons under graphene will introduce a gating effect, i.e. interfacial gating effect [26]. In this gating effect, the depletion layer (up to hundreds of nanometers thick) can act as dielectric layer, while the dielectric effect of the native oxide layer is negligible due to its ultrathin thickness. Since the lifetime of electrons generated in lightly doped Si is much longer than the transit time of carriers in graphene channel [19], high gain can be introduced and will greatly increase the photoresponse. Therefore, it is reasonable to attribute the high photoresponsivity of the device or ultrasensitive characteristic of the PSD to the synergistic effect of interfacial gating and charge injection.

4 Conclusions

In summary, we present an ultrasensitive PSD based on the graphene-Si hybrid structure by using synergistic effect. The holes generated in Si are directly transferred and injected into graphene to form photoresponse, while the electrons remaining in Si introduce a high gain through the interfacial gating effect. Both holes and electrons promote the photoresponse and position sensitivity. This PSD can operate under ultraweak light at the pW level for visible light and 1 nW for 1064 nm. At the same time, it retains fast response speed at μs level. This work therefore provides important advances and new development opportunity for future weak signal sensing.

Acknowledgments: This work was supported in part by the National Key Research and Development Program of China (No. 2017YFA0205700), NSFC (61774034, 11704068, Funder Id: <http://dx.doi.org/10.13039/501100001809>), the Strategic Priority Research Program of Chinese Academy of Sciences, Grant No. XDB30000000, China Postdoctoral Science Foundation (2018M632197, Funder Id: <http://dx.doi.org/10.13039/501100002858>), Funding of Natural Science Research Projects in Colleges and Universities of Jiangsu Province (18KJD140003), and the Fundamental Research Funds for the Central Universities (2242019R20025).

References

- [1] Cerezo A, Godfrey TJ, Smith GDW. Application of a position-sensitive detector to atom probe microanalysis. *Rev Sci Instrum* 1988;59:862–6.
- [2] Cao B, Hoang P, Ahn S, Kang H, Kim J, Noh J. High-speed focus inspection system using a position-sensitive detector. *Sensors* 2017;17:2842.
- [3] Liu K, Wang W, Yu Y, et al. Graphene-based infrared position-sensitive detector for precise measurements and high-speed trajectory tracking. *Nano Lett* 2019;19:8132–7.
- [4] Wang W, Liu K, Jiang J, et al. Ultrasensitive graphene-Si position-sensitive detector for motion tracking. *InfoMat* 2020. Doi:10.1002/inf2.12081.
- [5] Lucovsky G. Photoeffects in nonuniformly irradiated P-N junctions. *J Appl Phys* 1960;31:1088–95.
- [6] Liu Y, Liu J, Zhang Z, et al. Power-dependent lateral photovoltaic effect in a-Si: H/c-Si p-i-n structure at different temperatures. *Mater Lett* 2016;176:257–60.
- [7] Henry J, Livingstone J. A comparative study of position-sensitive detectors based on Schottky barrier crystalline and amorphous silicon structures. *J Mater Sci-Mat El* 2001;12:387–93.
- [8] Yu CQ, Wang H, Xia YX. Enhanced lateral photovoltaic effect in an improved oxide-metal-semiconductor structure of $\text{TiO}_2/\text{Ti}/\text{Si}$. *Appl Phys Lett* 2009;95:263506.
- [9] Chi L, Zhu P, Wang H, Huang X, Li X. A high sensitivity position-sensitive detector based on Au-SiO₂-Si structure. *J Optics* 2011;13:015601.
- [10] Yu CQ, Wang H, Xia YX. Giant lateral photovoltaic effect observed in TiO_2 dusted metal-semiconductor structure of $\text{Ti}/\text{TiO}_2/\text{Si}$. *Appl Phys Lett* 2009;95:141112.
- [11] Sarker BK, Cazalas E, Chung T, Childres I, Jovanovic I, Chen YP. Position-dependent and millimetre-range photodetection in phototransistors with micrometre-scale graphene on SiC. *Nat Nanotechnol* 2017;12:668–74.
- [12] Javadi M, Gholami M, Torbatiyan H, Abdi Y. Hybrid organic/inorganic position-sensitive detectors based on PEDOT:PSS/n-Si. *Appl Phys Lett* 2018;112:113302.
- [13] Hao L, Liu Y, Han Z, Xu Z, Zhu J. Large lateral photovoltaic effect in MoS_2/GaAs heterojunction. *Nanoscale Res Lett* 2017;12:562.
- [14] Hao LZ, Liu YJ, Han ZD, Xu ZJ, Zhu J. Giant lateral photovoltaic effect in $\text{MoS}_2/\text{SiO}_2/\text{Si}$ p-i-n junction. *J Alloy Compd* 2018;735:88–97.

- [15] Wang W, Du R, Guo X, et al. Interfacial amplification for graphene-based position-sensitive-detectors. *Light: Sci Appl* 2017;6:e17113.
- [16] Wang W, Yan Z, Zhang J, Lu J, Qin H, Ni Z. High-performance position-sensitive detector based on graphene–silicon heterojunction. *Optica* 2018;5:27.
- [17] Martins R, Fortunato E. Lateral photoeffect in large area one-dimensional thin-film position – sensitive detectors based in a-Si: H P-I-N devices. *Rev Sci Instrum* 1995;66:2927–34.
- [18] Liu F, Kar S. Quantum carrier reinvestment-induced ultrahigh and broadband photocurrent responses in graphene-silicon junctions. *ACS Nano* 2014;8:10270–9.
- [19] Chen Z, Cheng Z, Wang J, et al. High responsivity, broadband, and fast graphene/silicon photodetector in photoconductor mode. *Adv Opt Mater* 2015;3:1207–14.
- [20] Li X, Zhu H, Wang K, et al. Graphene-on-silicon Schottky junction solar cells. *Adv Mater* 2010;22:2743–8.
- [21] Song Y, Li X, Mackin C, et al. Role of interfacial oxide in high-efficiency graphene – silicon Schottky barrier solar cells. *Nano Lett* 2015;15:2104–10.
- [22] Yang L, Yu X, Hu W, Wu X, Zhao Y, Yang D. An 8.68% efficiency chemically-doped-free graphene–silicon solar cell using silver nanowires network buried contacts. *ACS Appl Mater Inter* 2015;7:4135–41.
- [23] Goossens S, Navickaite G, Monasterio C, et al. Broadband image sensor array based on graphene–CMOS integration. *Nat Photonics* 2017;11:366–71.
- [24] Akatsuka M, Sueoka K. Pinning effect of punched-out dislocations in carbon-, nitrogen- or boron-doped silicon wafers. *Jpn J Appl Phys* 2001;40:1240–1.
- [25] Huang X, Mei C, Gan Z, Zhou P, Wang H. Lateral photovoltaic effect in p-type silicon induced by surface states. *Appl Phys Lett* 2017;110:121103.
- [26] Guo X, Wang W, Nan H, et al. High-performance graphene photodetector using interfacial gating. *Optica* 2016;3:1066–70.
- [27] Hu C, Wang X, Miao P, et al. Origin of the ultrafast response of the lateral photovoltaic effect in amorphous MoS₂/Si junctions. *ACS Appl Mater Inter* 2017;9:18362–8.
- [28] Zhao X, Zhang L, Gai Q, Hu C, Wang X. High-performance position-sensitive detector based on the lateral photovoltaic effect in MoSe₂/p-Si junctions. *Appl Optics* 2019;58:5200–5.
- [29] Wang X, Zhao X, Hu C, et al. Large lateral photovoltaic effect with ultrafast relaxation time in SnSe/Si junction. *Appl Phys Lett* 2016;109:23502.
- [30] Xiao SQ, Wang H, Zhao ZC, Gu YZ, Xia YX, Wang ZH. Lateral photovoltaic effect and magnetoresistance observed in Co–SiO₂–Si metal–oxide–semiconductor structures. *J Phys D: Appl Phys* 2017;40:6926–9.

Supplementary Material: The online version of this article offers supplementary material (<https://doi.org/10.1515/nanoph-2020-0053>).